Direct observation of relaxation modes in KNbO$_3$ and BaTiO$_3$ using inelastic light scattering

J. P. Sokoloff*

Physics Department, Indiana University, Bloomington, Indiana 47401

L. L. Chase

Lawrence Livermore National Laboratories, Livermore, California 94550

D. Rytz

Hughes Research Laboratories, Malibu, California 90265

(Received 14 January 1988)

Cubic and tetragonal BaTiO$_3$ and orthorhombic KNbO$_3$ have been studied by Raman scattering, using an iodine filter to eliminate elastically scattered light. In addition to the usual phonon features, such as the soft E mode in tetragonal BaTiO$_3$ and the soft B_2 mode in orthorhombic KNbO$_3$, central components have been observed in both materials for the first time. These components have the linewidths, line shapes, and thermal properties of relaxation modes, and symmetry properties consistent with an eight-site order-disorder model of the successive phase transitions. Additionally, the data provide direct evidence that clusters of precursor order are present in cubic BaTiO$_3$ and the model provides estimates of the temperatures at which these clusters are present in both BaTiO$_3$ and KNbO$_3$. These values are in good agreement with the results of linear birefringence and refractive-index measurements.

I. INTRODUCTION

Two of the most extensively studied ferroelectric crystals are KNbO$_3$ and BaTiO$_3$, which have the ABO_3 perovskite structure. A major objective of these studies is to investigate the origin of the cubic-tetragonal-orthorhombic-rhombohedral sequence of structural phase transitions which these crystals undergo as they are cooled. In 1960, at an early stage in these studies, a lattice-dynamical soft-mode model was proposed in which components of a low-frequency cubic phonon mode become successively unstable and lead to a displacement of the equilibrium position of the B ion within the unit cell.[1,2] These displacements are along the $\langle 001 \rangle$ direction in the tetragonal phase, the $\langle 110 \rangle$ direction in the orthorhombic phase, and the $\langle 111 \rangle$ direction in the rhombohedral phase and thus account for the observed polarization direction in each phase. In this model the unstable normal mode (i.e., the soft mode) has a frequency which decreases as each transition temperature is approached (from above or below) and is described by the relation

$$\omega_s^2 = A(T - T_c) , \qquad (1)$$

where A is a constant and T_c is one of the transition temperatures.

This displacive model, in addition to explaining the sequence of phase transitions, was successful in other ways. For instance, Eq. (1), along with the Lyddane-Sachs-Teller (LST) relation

$$\epsilon(0) = \epsilon_\infty \frac{\omega_{LO}^2}{\omega_{TO}^2} \qquad (2)$$

which relates the high- (ϵ_∞) and low- [$\epsilon(0)$] frequency

dielectric constants to a particular optic mode's longitudinal (LO) and transverse (TO) frequencies, implies a divergence in $\epsilon(0)$ at T_c. In fact a Curie-Weiss behavior of the low-frequency dielectric function of the form

$$\epsilon(0) = \frac{C}{|(T - T_0)|} , \qquad (3)$$

where T_0 is the Curie-Weiss temperature and C is a constant, is observed.[3] Also, spectroscopic studies show that a zone-center phonon does decrease in frequency as each of the phase transitions is approached from above.[4-9]

Many studies however, display results inconsistent with this soft-mode model. The first of these came in 1968 when Comes, Lambert, and Guinier observed distinct sheets of unexpectedly diffuse x-ray scattering from the {100} reciprocal-lattice planes in BaTiO$_3$, KNbO$_3$, and the incipient ferroelectric KTaO$_3$ in all phases except the rhombohedral phase.[10] From these results Comes et al.[11] suggested a description of the phase transition based on the existence of local *static* disorder. They suggested that all phases but the rhombohedral phase are partially disordered; the disorder results from several possible statistical orientations of the central B ion at one of eight sites which are located off center along different $\langle 111 \rangle$ directions. Although it was pointed out that this result could be a consequence of the strong anisotropy of the frequency versus wave-vector dispersion of the lowest-energy TO-phonon branch in these crystals,[12] subsequent studies also revealed evidence both in favor of disorder, and in contradiction to the soft-mode model. Infrared-reflectivity (IR) and Raman studies show that just below the two higher-temperature transitions the soft mode does *not* behave according to Eq. (1). Its general behavior is that it decreases continuously with decreasing

temperature through the first two transitions and increases only below the third transition, the ortho-rhombic-rhombohedral transition. Furthermore the soft mode in BaTiO$_3$ approaches a constant frequency $v_s \simeq 60$ cm^{-1} at about 100 °C above T_{c1}, the cubic-tetragonal transition temperature, and does not begin decreasing again until below T_{c1}.[13] These results imply that in the vicinity of T_{c1} there is some mechanism other than a soft phonon which contributes to the observed divergence in $\epsilon(0)$ described qualitatively by Eq. (3). In fact, dielectric measurements indicate that the phonons in these crystals cannot at all account for the observed low-frequency dielectric constant near the first transition. There are observed discrepancies between $\epsilon(LST)$, the value of $\epsilon(0)$ deduced using a generalized form of Eq. (2) with spectroscopically determined phonon frequencies, and the value measured directly by capacitance techniques, $\epsilon(cap)$, which is largest near the upper frequency limit of capacitance measurements.[14–17] This discrepancy is largest just above the cubic-tetragonal transition in BaTiO$_3$.[18,19] This suggests that there is a contribution to $\epsilon(cap)$ from a relaxation mechanism with a characteristic frequency greater than the mechanical resonances, but below optic-phonon resonances. In addition to the original x-ray, spectroscopic, and dielectric studies mentioned above, refractive-index measurements,[20–22] hyper-Raman scattering studies,[23–26] and more recent x-ray measurements[27,28] also indicate that there is some structural disorder present in the cubic phase of these crystals.

The relaxation modes responsible for the contribution to the dielectric constant $\Delta\epsilon = \epsilon(cap)-\epsilon(LST)$, and which presumably involve motion by the ions among the sites of a disordered sublattice, have characteristic relaxation times in the range 10^{-9}–10^{-12} sec and are therefore difficult to probe using conventional spectroscopic methods. Such low-frequency phenomena however can be directly observed in light scattering spectra, and will appear as a "central peak" (CP) if an iodine filter is employed to absorb the intense elastically scattered light. Central peaks have been seen in glasses[29] and other materials,[30–32] and in the case of a glass their presence is related to the innate structural disorder. More recently a central peak has been seen in KTa$_{0.72}$Nb$_{0.28}$O$_3$ (KTN) and has been taken as evidence of disorder in a perovskite structure.[33] It is possible, however, that the disorder in KTN can be attributed to its mixed crystal nature. In order to determine if this disorder is intrinsic to the ferro-distortive perovskite structure a similar search for spectral central peaks, the results of which we report here, was undertaken in BaTiO$_3$ and KNbO$_3$.

II. EXPERIMENTAL

The light-scattering spectra were obtained using the 5145-Å line of an argon laser tuned to the absorption of an I$_2$ filter, which completely eliminated the elastically scattered light. All experiments were carried out in a right-angle scattering geometry and the Raman and quasielastic components were dispersed by either a double monochromator or by a triple-pass Fabry-Perot interferometer followed by a double monochromator.[34]

The anisotropic nature of the tetragonal and ortho-rhombic phases of KNbO$_3$ and BaTiO$_3$ imposes strict light-scattering selection rules which depend on the symmetry of the crystal excitations and the point group of the crystalline phase. For instance, KNbO$_3$ was studied in its orthorhombic phase where all excitations at zero wave vector transform according to either the $A_1(c)$, $B_2(b)$, $B_1(a)$, or A_2 irreducible representations of the C_{2v} point group. Here a,b,c are the orthorhombic phase principal axes, which differ from the pseudocubic axes by a $\pi/4$ rotation about the $\hat{y}\|[010]$ pseudocubic axis. The pseudocubic axes (x,y,z) are used as the principal axes in the tetragonal and cubic phases with the $\hat{z}\|[001]$ direction chosen for the tetragonal polar axis. Figure 1 shows the two sets of principal axes. The scattering configurations, as well as the symmetry of the excitations probed by each configuration, are given in Table I. Polar modes which are not simultaneously polarized along a principal axis and pure-transverse or pure-longitudinal modes become mixed in symmetry due to a competition between ionic and electrostatic forces, which for this case, are not colinear. For instance, the $a(cc)b$ scattering geometry, in which the wave-vector transfer is perpendicular to the polar c axis, can be employed in orthorhombic KNbO$_3$ to study pure A_1-symmetry modes but not pure B_1- or B_2-symmetry excitations. Pure B_2-symmetry modes however, can be studied in the $a(bb)c$ scattering configuration. These symmetry features of the different scattering configurations are also indicated in Table I.

The BaTiO$_3$ samples were studied in both the cubic and tetragonal phase. When studied in the tetragonal phase they were first poled along the z axis with a field $\simeq 5$ kV/cm and lowered below the cubic-tetragonal transition temperature, in order to obtain a single-domain tetragonal phase sample. The point group of the tetragonal phase is C_{4v} and the excitations of major interest are low-frequency E-symmetry modes, in which ionic displacements are perpendicular to the polar axis, and A_1-symmetry modes, which involve ionic motion parallel to the polar axis.
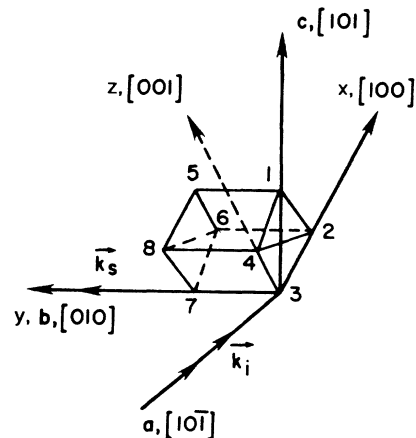

FIG. 1. The cubic and tetragonal (x,y,z), and orthorhombic (a,b,c) principal axes, relative to the pseudocubic $(\langle 100 \rangle)$ axes.

TABLE I. Scattering geometrics. k and ϵ are the propagation and polarization directions of the incident (i) and scattered (s) light. The symmetry of the probe excitation (mode), as well as the mode each is mixed with, is also given.

	$k_i(\epsilon_i\epsilon_s)k_s$	Symmetry (mixed)
Orthorhombic	$a(cc)b$	A_1
KNbO₃	$a(ca)b$	B_1 $(+B_2)$
	$a(bc)b$	B_2 $(+B_1)$
	$a(ba)b$	A_2
	$a(cb)c$	B_2
Tetragonal	$x(zx)y$	E
BaTiO₃	$x(zz)y$	A

III. EXPERIMENTAL RESULTS

A. Orthorhombic KNbO₃

Figure 2 shows the results of Raman scattering in orthorhombic KNbO₃ at $T=30$ and $180\,°$C. A single-domain sample, grown at Hughes Laboratories by the top-seeded solution method[35] and stable between -50 and $220\,°$C, was used to make these measurements. The usual elastic spectral response has been eliminated by the I_2 filter thus allowing an unobscured view of all low-frequency features. The phonons in these spectra have
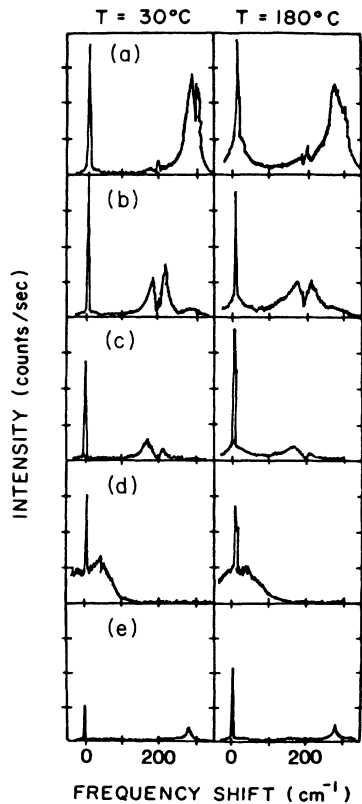

FIG. 2. Raman scattering in orthorhombic KNbO₃ at $T=30\,°$C and $T=180\,°$C: (a) A_1 spectra [$a(cc)b$]; (b) mixed B_1 spectra [$a(ca)b$]; (c) mixed B_2 spectra [$a(bc)b$]; (d) B_2 spectra [$a(cb)c$]; (e) A_2 spectra [$a(ba)b$]. Resolution is 2 cm^{-1}.

frequencies which are in good agreement with previous Raman studies.[36,37] Lattice-dynamical studies[38] show that the broad A_1 symmetry phonon at $v=283$ cm^{-1}, the broad B_2 phonon with a maximum at $v=60$ cm^{-1} (in the $T=30\,°$C spectrum), and the B_1 phonon in the mixed (B_1+B_2)-symmetry spectra all derive from the low-frequency cubic phase F_{1u} phonon mode characterized by motion of the Nb ion against the rigid oxygen octahedron. The shift of the low-frequency B_2(TO) phonon from $v=60$ cm^{-1} [Fig. 2(d)] out to $v=170$ cm^{-1} in the B_1+B_2 mixed symmetry spectra [Figs. 2(b) and 2(c)] is due to the large anisotropy in the phonon energy-versus-wave-vector dispersion.[39]

Three features of Figs. 2(a)–2(c) indicate that there is dynamic disorder among the Nb ions at high temperatures. First, there is a clear broadening of the spectral response of the phonons mentioned above in the $T=180\,°$C spectra compared to the $T=30\,°$C spectra. These are the phonons which, as noted above, involve Nb ion displacements. The presence of broad phonons is often a consequence of general translational disorder. This, together with the fact that the nonpolar A_2 phonon mode [Fig. 2(e)], which involves only oxygen ions, has no temperature dependence implies disorder among the Nb ions. Second, there is a significant increase in the Raman background between 0 and $\simeq 300$ cm^{-1} at high T. A broad background has been seen in KNbO₃ by other researchers[36,37] and is believed to be due to disorder induced scattering rather than second-order Raman scattering. Third, at higher T pronounced quasielastic scattering, i.e., a central peak (CP), is present. This is the first reported observation of a CP feature in KNbO₃, and suggests that there is a low-frequency thermally activated relaxation process in orthorhombic KNbO₃ involving the Nb ion. One such relaxation process, which is inherently order-disorder in character and therefore consistent with the other two disorder features, is an orientational process in which the Nb ion moves from one equilibrium site to another in a multiwell potential, and on a time scale long compared to inverse phonon frequencies. This process would produce a central peak characteristic of a Debye relaxation. A last important point is that the low-frequency B_2(TO) phonon [Fig. 2(d)], which has a polarization parallel to the b axis, shows no evidence of any of the disorder features noted in the spectra of Figs. 2(a)–2(c). On the contrary, this phonon displays a soft-mode behavior; it has a spectral response well described by a heavily damped harmonic oscillator with a temperature-dependent frequency, and can be adequately described as motion by the Nb ion within a quasiharmonic single-well potential. We therefore conclude that there is dynamic disorder present in KNbO₃ with directional properties. In particular, there is disorder along the polar axis as indicated by the A_1-symmetry spectra and disorder in the ab plane as indicated by the mixed (B_1+B_2)-symmetry spectra. However, the single-well description for the B_2 spectra indicates that there is *no* disorder along the b axis, the direction of soft-mode displacements in the orthorhombic phase.

Further evidence of dynamic disorder with directional

properties is provided by the data collected using the Fabry-Perot (FP) interferometer. FP spectra were collected in all configurations listed in Table I. In all cases a Brillouin doublet, unaffected by temperature, and similar to the doublet shown in Fig. 3(a) (and which is unresolved in the Raman data) was seen. However, only in the A_1-symmetry spectra [i.e., the $a(cc)b$ configuration] a narrow peak of full width at half-maximum (FWHM) $\simeq 5$ GHz was also observed. This is shown in Fig. 3(b) without the accompanying Brillouin doublet at ± 30 GHz. This narrow CP, like the broader CP, was more intense at higher temperatures, but at $T = 180\,°C$ it was still about a factor of 20 less intense than the Brillouin components. Because the width of this narrow peak is on the order of the FP interferometer resolution, its presence could, in principle, simply be due to the transmission of a small amount of elastically scattered light. However, this narrow component appeared in data runs taken at different I_2 filter attenuations and so is due to a low-frequency excitation in the crystal rather than elastic scattering. Furthermore, because the I_2 absorption line is on the order of 1 GHz in width it is possible that a large amount of inelastically scattered light of small frequency shifts (< 1 GHz), as well as the elastic scattered light, is absorbed by the I_2 filter. In this case the low intensity CP's in Fig. 4 would be only the tails of more intense peaks.

To summarize, there is evidence of dynamic disorder in the Nb sublattice in orthorhombic $KNbO_3$. In particular, the A_1 and ($B_1 + B_2$) mixed-symmetry Raman spectra contain broadened phonons and a substantial low-frequency Raman background at high temperatures. Additionally CP's of two different widths were also seen in the A_1-symmetry spectra, which is suggestive of two relaxation modes with different time scales involving motion along the polar axis. Another CP in the mixed symmetry ($B_1 + B_2$) spectra is suggestive of a relaxation mode involving motion in the ab plane, but because of the damped harmonic response of the low-frequency B_2(TO) phonon, relaxation does not occur along the b axis. Neither the narrow A_1-symmetry CP of FWHM $\simeq 5$ GHz nor either of the broad CP's of FWHM $\simeq 20$ cm^{-1} have

FIG. 4. Raman scattering in cubic and tetragonal BaTiO$_3$; (a) E-symmetry spectra $[x(zx)y]$ containing the overdamped soft mode; (b) A-symmetry spectra $[x(zz)y]$ containing a broad CP.

been seen before in previous light scattering measurements which did not use an I_2 filter. These features extend the observed light scattering spectrum down to frequencies still above, but closer to, the upper limits of dielectric measurements. Although the available high-frequency capacitance data are limited, they are consistent with the present data. For instance, anomalous dispersion in the microwave regime, which was observed along the c axis only, corresponds to the observed narrow A_1-symmetry CP. Similarly, the fact that no microwave dispersion was observed along the a or b axis is in agreement with the absence of a narrow CP of B_1 or B_2 symmetry.[15]

B. BaTiO$_3$

The Raman and infrared responses of BaTiO$_3$ have been studied in great detail. In the tetragonal phase the low-frequency spectrum contains the $A_1 + E$ components of the lowest-energy cubic phase F_{1u} soft mode. These modes are completely analogous to the A_1 and soft B_2 modes (at $v = 283$ and 60 cm^{-1}, respectively) in orthorhombic KNbO$_3$, with the soft E mode in BaTiO$_3$ being even more heavily damped than the orthorhombic B_2 soft mode in KNbO$_3$. Additionally, three A_1-symmetry broad phonons observed in the Raman scattering experiments in both the tetragonal and cubic phases have been extensively studied and discussed.[7,40-42]

Figure 4 shows the first low-frequency E-symmetry and A-symmetry Raman spectra of BaTiO$_3$ taken with an I_2 filter. A BaTiO$_3$ sample grown by the top-seeded solution
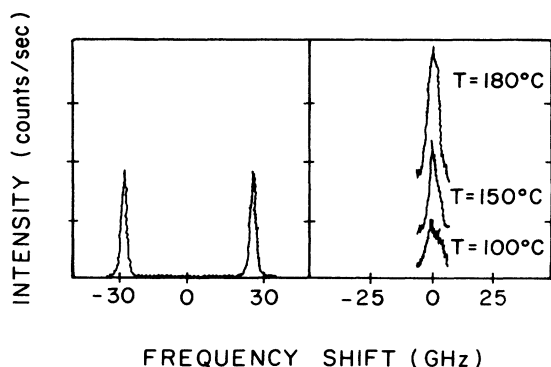

FIG 3. Fabry-Perot data of orthorhombic KNbO$_3$: (a) Brillouin doublet typical in all spectra; (b) CP in A_1 spectrum. Resolution is 2 GHz.
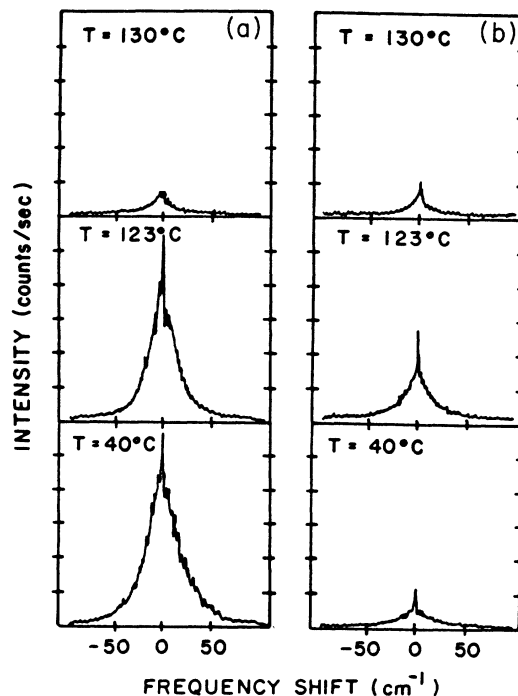
method by the Sanders Company in Nashua, New Hampshire and determined to have a cubic-tetragonal transition temperature of $T_{c1} = 124\,°C$, was used for these measurements.[43] These E- and A-symmetry Raman spectra are in many ways similar to the B_2- and A_1-symmetry Raman spectra in orthorhombic KNbO$_3$. Below T_{c1} the E-symmetry spectrum [Fig. 4(a)] contains a heavily damped soft mode which appears in the FP E-symmetry spectra of Fig. 5(a) as a large background. The low-frequency A_1-symmetry spectrum is also similar to the A_1-symmetry spectrum in orthorhombic KNbO$_3$. The Raman spectrum in Fig. 4(b) contains a CP of FWHM of ~ 20 cm^{-1} while the FP spectrum contains a narrow CP with a FWHM of several GHz. Like the A_1-symmetry CP's in orthorhombic, KNbO$_3$ these CP's decrease in intensity with decreasing temperature. It is not likely that the broad A_1-symmetry CP seen in the Raman data is actually spectral leakage of the much higher intensity E-symmetry soft mode resulting from slight analyzer, polarizer, or crystal misorientation since the line shape of this central component in the A_1-symmetry Raman spectra is *not* the same as that of the E soft mode. Furthermore, an explanation of spectral leakage does not account for the observed thermal behavior.

These two A_1-symmetry CP's are indications of dynamic disorder of the Ti ions, along the polar axis of tetragonal BaTiO$_3$, with two different time scales. On the other hand, the presence of an overdamped E-phonon response, rather than a CP response, suggests that ionic motion in the xy plane is characterized by motion of the Ti ion in an anharmonic single-well local potential, rather than a double-well potential (DWP) with minima along the z axis which could explain the relaxation response of the z-polarized Ti motion.

Further evidence of disorder can be seen in the spectra of Figs. 4 and 5 taken above T_{c1} in the cubic phase. Not only do both the broad and narrow CP persist [Figs. 4(b)

and 5(b)], but in Fig. 4(a) the overdamped soft E phonon which is Raman inactive above T_{c1}, is replaced by a narrower, less intense CP identical to the cubic-phase CP seen in Fig. 4(b). The full thermal evolution of this broad cubic-phase CP is shown in Fig. 6. This cubic phase CP, which both narrows and increases in intensity with decreasing temperature, is similar to CP behavior reported in cubic KTa$_{0.72}$Nb$_{0.28}$O$_3$ (Ref. 33) which is discussed elsewhere.[44]

In summary, a narrow CP of FWHM of ~ 5 GHz and a broad CP with a FWHM about 2 orders of magnitude larger were observed in tetragonal BaTiO$_3$. The intensities of these CP's decreased with decreasing temperature. Furthermore, these low-frequency features, like the CP's seen in orthorhombic KNBO$_3$, have A_1 symmetry, which implies that there are relaxation modes involving interwell motion by Ti ions parallel to the polar axis. Conversely the E-symmetry low-frequency spectra were completely consistent with all other investigations of the soft E mode in tetragonal BaTiO$_3$, and indicate that the motion of the Ti ions in the xy plane is best described as a heavily damped phonon mode. Both the A_1 CP features persisted into the cubic phase, where the broad CP, in particular, both broadened in width and decreased in intensity as the temperature was increased.

The presence of the CP responses in BaTiO$_3$ is direct evidence that a relaxation mechanism is present in BaTiO$_3$. Such a suggestion is not new. For instance, in tetragonal BaTiO$_3$ relaxation processes have been proposed to explain the discrepancy between ϵ(LST) and ϵ(cap) when measured along the z axis.[45] Also, as mentioned above, broad A_1-symmetry phonon features, which like the A_1-symmetry CP's in the present data persist into the cubic phase, have been taken as evidence of disorder and explained by some researchers as a result of interwell tunneling parallel to the z axis by the Ti ions in tetragonal BaTiO$_3$.[46]

A possible origin of the central peak components observed in the cubic phase is that they are due to scatter-

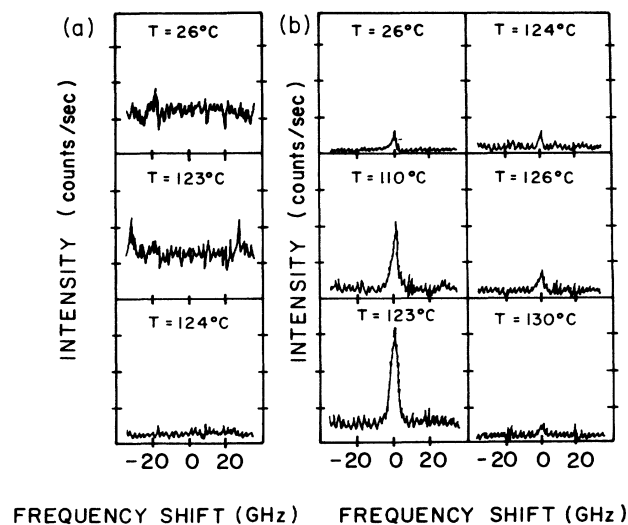FIG. 5. Fabry-Perot data of cubic and tetragonal BaTiO$_3$: (a) E-symmetry spectra; (b) A-symmetry spectra.

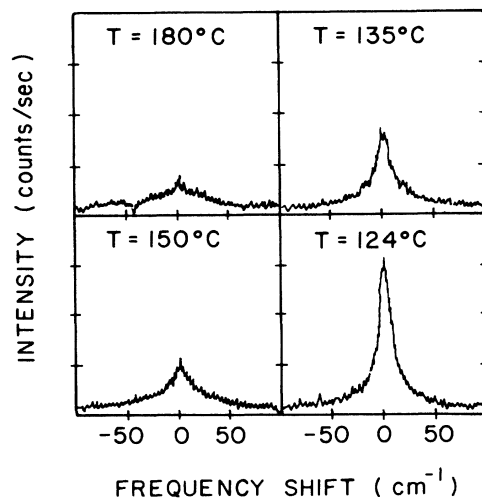FIG. 6. Raman scattering in cubic BaTiO$_3$ [$x(zx + zz)y$].

ing from regions of precursor order. Theoretical studies,[47-49] which for the most part have been carried out in one or two dimensions, predict the appearance of such precursor clusters. Furthermore, numerous other experiments have displayed results which could be explained by the presence of clusters which have tetragonal ordering. For instance, a temperature-dependent dielectric response at $\simeq 1$ cm^{-1} is present which is not due to phonon resonances.[17-19] Hyper-Raman scattering experiments in cubic BaTiO$_3$.[24,25] KNbO$_3$,[26] KTaO$_3$,[50] and KTN (Ref. 51) display a second harmonic generation signal which is forbidden in crystals of perfect cubic symmetry. Also, refractive index measurements show a deviation in the refractive index from the expected linear dependence on T expected in cubic crystals.[21,22] Like the central peak in these experiments, all of these anomalous quantities increase dramatically as the phase transition is approached from above, and suggest the presence of a volume of precursor clusters which grows as T_{c1} is approached from above.

IV. THE EIGHT-SITE MODEL

To explain the light scattering features observed in these experiments we introduce a modified version of the eight-site (ES) model originally proposed in 1968 by Comes et al.[10,11] In the present single-particle model the B ion of the ABO_3 perovskite structure is located off center in an eight-well potential which has each site (i.e., potential minimum) displaced from the unit cell center along a $\langle 111 \rangle$ direction. The different phases are a consequence of preferential occupation by the B ion of a certain set of sites. In the cubic phase the occupation of each of the eight sites is the same. Below the first transition temperature preferential occupation of a set of four potential sites perpendicular to a particular axis results in tetragonal ordering. Below the second transition temperature two sites on a line parallel to a cube edge are most populated leading to the orthorhombic phase. Finally, below the third transition temperature occupation of only one of the off-center sites is favored resulting in the rhombohedral phase. The orientation of the eight-site potential relative to the principal axes in both the orthorhombic phase, and tetragonal and cubic phases is shown in Fig. 1.

While it is the relative site occupations that determine the crystal phase, it is the nature of the intersite and intrasite motion that determines the spectral response. This motion is, of course, determined by the height of the energy barriers separating the different sites (i.e., the activation energy) and, in the case of the three lower phases, the energy difference between energetically inequivalent sites. Figure 7 shows the potential along a line through two sites when the line is either perpendicular [Fig. 7(a)] or parallel [Fig. 7(b)] to the polar axis. In this figure E_0 is the zero-point vibrational energy of the B ion, V_0 is the potential barrier, and U is a potential difference resulting from the macroscopic polarization within the crystal. For motion in the symmetric potential of Fig. 7(a), if V_0 is of a magnitude such that thermal excitations allow the B ion to move between these two sites of the lo-
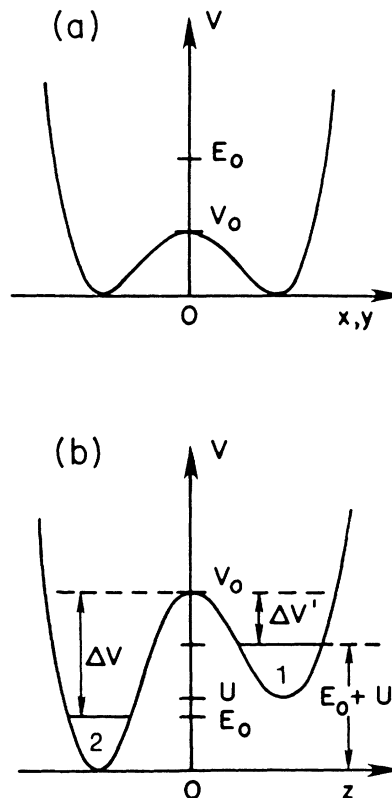

FIG. 7. Local potential along a line through two sites in the eight-site potential which is (a) parallel to a nonpolar principal axis and (b) parallel to the ferroelectric axis.

cal potential on a time scale comparable to the inverse of a typical lattice vibration then the ionic motion and spectral response will be that of a damped phonon mode

$$S(v) \propto \frac{v\Gamma}{(v_0^2-v^2)^2+v^2\Gamma^2} \ . \tag{4}$$

On the other hand, if V_0 is of a magnitude such that interwell motion occurs on a time scale long compared to the inverse of even a low-energy phonon frequency, then the motion is best described as a Debye relaxation and the spectral response will be the characteristic Lorentzian centered on zero-frequency shift with a half-width at half maximum (HWHM) approximately equal to the average B ion relaxation or "dwell" time, τ,

$$S(v) \propto \frac{1}{1+v^2\tau^2} \ . \tag{5}$$

Similarly the nature of the ionic motion between the biased wells [Fig. 7(b)] depends on the magnitude of V_0 and U. If these values are such that the B ion is mostly confined to the low-energy well, then the motion is predominantly vibrational. However, relaxation modes involving motion between inequivalent wells will occur. Such relaxations will be characterized by two dwell times describing the average time spent by the ion in each potential well and the spectral response will correspondingly be composed of two Lorentzians with HWHM's ap-

proximately equal to the inverse of the dwell times.

In the KNbO$_3$ low-frequency spectra of the two A_1-symmetry CP's are due to relaxation modes involving ionic motion along the orthorhombic, polar c axis. The broad (narrow) A_1 CP has a HWHM of $\sim(1/\tau_1)$ $[(1/\tau_2)]$, where τ_1 (τ_2) is the average dwell time of the B ion in the upper (lower) well before it goes into the lower (upper) well, and of course, $\tau_1 < \tau_2$ since the low-energy well is the energetically favorable one. The overdamped B_2 phonon is due to motion by the Nb ion parallel to the b axis. In this case the energy barrier V_0 perturbs the harmonic motion but not so much that the motion is still not vibrational. Finally, the mixed $(B_1 + B_2)$-symmetry CP's are due to interwell motion in the ab plane, but not along the b axis, and in this case the potential barriers separating the different sites are such that the interwell motion is more like a relaxation mode, rather than a damped vibration.

In the case of BaTiO$_3$ the two A_1-symmetry CP's are again a result of relaxations along the polar axis and between the energetically inequivalent sites. The E-symmetry overdamped phonon is the spectral response associated with the vibrational motion when the Ti ion moves in an xy plane containing either set of four energetically equivalent sites. In this case, as in the case of the B_2 mode in orthorhombic KNbO$_3$, the potential barriers separating any two of the four sites in the same xy plane perturb the harmonic motion. However, the motion is still vibrational in character. In cubic BaTiO$_3$ the CP response is due to scattering from the ionic motion within regions containing precursor clusters. The total volume of the precursor clusters increases as $T \to T_{c1}^+$ and this accounts for the increase in intensity.

To describe the relaxation mode more precisely we use the tunneling model which has been applied to both spectroscopic and dielectric data in tetragonal BaTiO$_3$. In this semiclassical model[45] the thermally excited B ion tunnels through the top of a barrier confining it to a particular set of sites. The average dwell or relaxation time in this set of sites can be written

$$\tau = \tau_0 \exp\left[\frac{(\Delta V - kT)}{kT_0}\right] . \qquad (6)$$

Here ΔV is defined in Fig. 7(b) as the height of the barrier, $E = \langle E \rangle = kT$ is the average B ion energy, $kT_0 = (\hbar/2\pi) \sqrt{\alpha/m_B}$ is related to the mass m_B of the B ion and the curvature α of the potential barrier. $(\tau_0)^{-1}$ is a tunneling "attempt" frequency and a typical physically plausible value for this quantity is several hundred cm^{-1}. Simple arguments allow the total broad A_1 CP intensity (i.e., the integrated intensity) as a function of temperature to be written. The total broad A_1 CP intensity I_1 is proportional to $N_{1 \to 2}$ relaxation events per unit time in which the B ion goes from well 1 to 2 $(1 \to 2)$. The relative occupations of well 1 and 2 are related by the Boltzmann factor

$$n_1 = n_2 \exp\left[\frac{-U}{kT}\right] .$$

Therefore,

$$\left| I_1 \propto N_{1 \to 2} = \frac{n_1}{\tau_1} \right| = \frac{n_2}{\tau_1} \exp\left[\frac{-U}{kT}\right] . \qquad (7)$$

In the ferroelectric phases the polarization of KNbO$_3$ and BaTiO$_3$ changes very little so n_2 can be considered constant, and we can relate the experimentally determined quantities I_1 and τ_1 to the potential bias U

$$I_1 \tau_1 = C \exp\left[\frac{-U}{kT}\right] , \qquad (8)$$

where C is a constant. Equation (8) is based only on the argument that there is a relaxation process present involving intersite motion by an ion between inequivalent sites. The goodness of the fits of data to Eqs. (6) and (8), as well as resulting values for ΔV and U, will be an indication of the plausibility of the tunneling model and the eight-site model in general.

V. RESULTS AND CONCLUSIONS

In analyzing the CP data we first see if they have the relaxation line shape described by Eq. (5), and then if the values of τ and I_1 have thermal dependences which can be fitted to Eqs. (6) and (8). The spectra which we consider are, first, the broad A_1-symmetry CP in orthorhombic KNbO$_3$ and second, the CP observed in cubic BaTiO$_3$ (Fig. 6). The broad A_1-symmetry CP in orthorhombic KNbO$_3$ was more intense than the $B_1 + B_2$ mixed-symmetry CP, and was less distorted by the low-frequency background and broad wing of the TO phonon. Therefore the fits of Eq. (5) to this data, some of which are shown in Fig. 8, yielded more reliable values.

The broad A_1-symmetry CP data in tetragonal BaTiO$_3$ were not analyzed because, although the intensity of this CP does decrease with decreasing temperature as would be expected in this model, slight spectral leakage of the
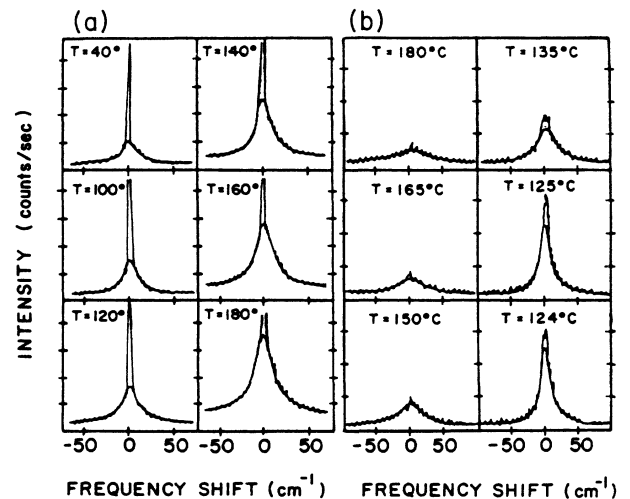

FIG. 8. A least-squares fit of Eq. (5) to the low-frequency region of the (a) A_1-symmetry Raman spectra in orthorhombic KNbO$_3$ and (b) Raman spectra in cubic BaTiO$_3$.

high-intensity overdamped E phonon into these spectra distorted the CP line shape and prevented accurate values of τ from being obtained. In the cubic $BaTiO_3$, however, this soft phonon is Raman inactive, it does not contaminate the CP spectra, and this allows the determination of a reliable set of values of τ. Since these CP's in cubic $BaTiO_3$ are due to relaxation events within a temperature-*dependent* volume of precursor clusters the expected thermal behavior of the CP intensity is unclear. It may not have the dependence on T described by Eq. (8), which is for a crystal composed of unit cells all of the same phase. If we make the assumption that any potential barriers and potential biases in a unit cell in a precursor cluster are temperature *independent*, any tunneling relaxation events within these clusters will have relaxation times describable by Eq. (6). We note that this assumption is consistent with the first-order nature of the cubic-tetragonal phase transition in $BaTiO_3$; presumably any changes in the local potential of an individual unit cell undergoing this phase transition will also be first order, even when this transition occurs locally, as in the case with a precursor cluster.

In Figs. 9(a) and 9(b) we show the results of fits of Eq. (6) to the relaxation times derived from both sets of spectra mentioned above, and in Fig. 9(c) is the result of a fit of the product of the values of I and τ to Eq. (8). The fit in Fig. 9(c) is based only on the assumption that there is a relaxation process present in orthorhombic $KNbO_3$ involving motion by the Nb ion between energetically inequivalent sites composing the order-disorder sublattice. The fitted value of U is 1150 cm$^{-1} \simeq 0.15$ eV, and is the right order of magnitude expected for single-particle ionic excitations. Turning to the fits in Figs. 9(a) and 9(b), we obtain values of $\Delta V = 750$ cm^{-1}, $kT_0 = 145$ cm^{-1} for $KNbO_3$, and $\Delta V = 400$ cm^{-1}, $kT_0 = 36$ cm^{-1} for $BaTiO_3$. The fits are very good and much better than Arrhenius-type fits to the data, although at high temperatures ($T > 120 °C$) the $KNbO_3$ data could be fit almost as well to a Arrhenius behavior. Notice that for both cases the barrier height is comparable to, but larger than, all thermal energies at which measurements were made. This is consistent with the model in which the thermally excited B ions have energies near, but below, the top of the potential barrier and then tunnel through the barrier. The value $\Delta V = 400$ cm^{-1} for $BaTiO_3$ corresponds to a temperature $\simeq 300 °C$, and thus places an upper limit to the temperature at which this tunneling process predominates. This maximum value of $300 °C$ is in excellent agreement with Burns' data[22] which show that at about $300 °C$ deviations in the refractive index from a linear dependence on T, and which can be associated with the presence of polarization in the cubic phase of $BaTiO_3$, first begin appearing. Similarly, the value of $\Delta V = 750$ cm^{-1} for $KNbO_3$ corresponds to an upper-limit temperature $\simeq 1070$ K at which the eight-site potential would be expected to localize the Nb ion off center. This is close to a maximum temperature of $\simeq 1000$ K that deviations from the expected high-temperature linear birefringence values have been seen in cubic ($T_{c1} = 705$ K) $KNbO_3$,[20] and these "birefringent tails" have been interpreted as
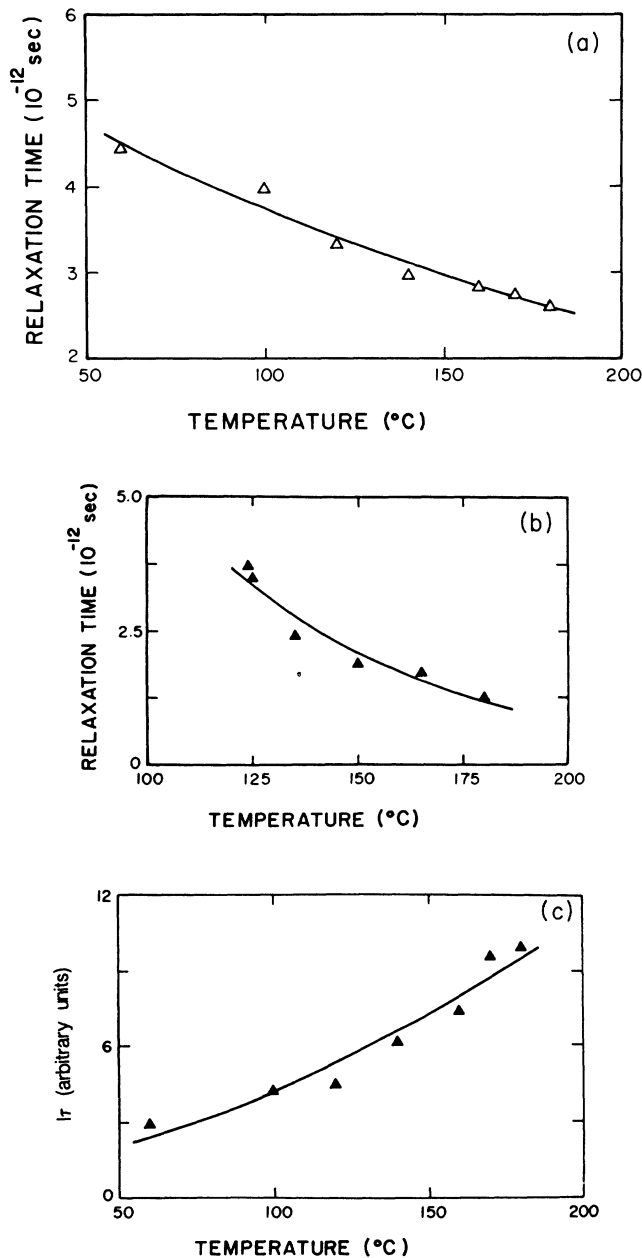

FIG. 9. (a) A fit of the relaxation times in orthorhombic $KNbO_3$ and tetragonal precursor clusters in cubic $BaTiO_3$ to a tunneling relaxation process in an eight-site potential [Eq. (6)]. (b) A fit of the product of the measured values of I and τ to the expected thermal behavior of the dynamic order-disorder events in orthorhombic $KNbO_3$ [Eq. (8)].

evidence of precursor clusters in cubic $KNbO_3$. Finally we note that all values of ΔV and U are comparable to typical activation energies for relaxation modes in ionic conductors. In this context it is worth mentioning that "dwell-dwell" models have been suggested to explain the different width central peaks seen in I_2 filter light scattering experiments on the ionic conductor $RbAg_4I_5$.[52]

In conclusion, we have observed for the first time central peak features in the Raman scattering spectra of or-

thorhombic KNbO$_3$,[53] and cubic and tetragonal BaTiO$_3$. These CP's have line shapes characteristic of Debye relaxation modes. The thermal dependence of the CP HWHM and integrated intensity, as well as the symmetry features of these CP's, are consistent with a model in which the central ion in the unit cells tunnels between certain sites of an eight-well potential. This model has also been successfully applied to Raman data collected on several KTN samples.[44]

*Present address: Optical Sciences Center, University of Arizona, Tucson, AZ 85721.

[1]W. Cochran, Adv. Phys. 9, 387 (1960).

[2]P. W. Anderson, Izv. Akad. SSR Nauk (Moscow) (1960).

[3]See, for instance, F. Jona and G. Shirane, Ferroelectric Crystals (Pergamon, New York, 1962).

[4]J. L. Servoin, F. Gervais, A. M. Quittet, and Y. Luspin, Phys. Rev. B 21, 2038 (1980).

[5]M. D. Fontana, G. Metrat, J. L. Servoin, and F. Gervais, J Phys. C 16, 483 (1984).

[6]G. Metrat, M. D. Fontana, and J. L. Servoin, Ferroelectric Lett. 44, 241 (1983).

[7]B. Jannot, L. Gnininvi, and B. Godefroy, Ferroelectrics 37, 669 (1983).

[8]M. D. Fontana, G. E. Kugel, G. Metrat, and C. Carabatos, Phys. Status Solidi B 103, 211 (1981).

[9]T. Shigenari, Phys. Lett. 98A, 63 (1983).

[10]R. Comes, M. Lambert, and A. Guinier, C. R. Acad. Sci. Paris 226, 959 (1968).

[11]R. Comes, M. Lambert, and A. Guinier, Solid State Commun. 6, 715 (1968).

[12]A. Huller, Solid State Commun. 7, 589 (1969).

[13]Y. Luspin, J. L. Servoin, and F. Gervais, J. Phys. C 13, 3761 (1980).

[14]A. V. Turik and N. B. Shevchenko, Phys. Status Solidi B 95, 585 (1979).

[15]A. V. Turik, N. B. Shevchenko, V. F. Zhestkov, V. G. Smotrakov, and E. G. Fesenko, Fiz. Tverd. Tela (Leningrad) 21, 1224 (1979) [Sov. Phys.—Solid State 21, 710 (1979)].

[16]R. Clemens, G. Luther, and H. E. Muser, Phys. Status Solidi A 64, 637 (1981).

[17]S. H. Wemple, M. D. Domenico, Jr., and I. Camlibel, J. Phys. Chem. 29, 1797 (1968).

[18]T. S. Benedict and J. L. Durand, Phys. Rev. 109, 1091 (1958).

[19]Y. M. Poplavko, Proceedings of the International Meeting on Ferroelectricity, 1966, Vol. II, p. 171, as cited in Ref. 13.

[20]W. Kleemann, F. J. Schafer, and M. D. Fontana, Phys. Rev. B 30, 1148 (1984).

[21]Gerald Burns and F. H. Dacol, Ferroelectrics 37, 661 (1981).

[22]Gerald Burns and F. H. Dacol, Solid State Commun. 42, 9 (1982).

[23]K. Inoue and S. Akimoto, Solid State Commun. 46, 441 (1983).

[24]H. Vogt, J. A. Sanjurjo, and G. Rossbroich, Phys. Rev. B 26, 3094 (1982).

[25]H. Vogt, M. D. Fontana, G. E. Kugel, and P. Gunter, Phys. Rev. B 34, 410 (1986).

[26]H. Uwe and H. Vogt, Ferroelectrics 55, 87 (1984).

[27]K. Itoh, L. Z. Zang, E. Nakamura, and N. Nishima, Ferroelectrics 63, 29 (1985).

[28]K. H. Ehses, H. Bock, and K. Fischer, Ferroelectrics 37, 507 (1981).

[29]P. A. Fleury and K. B. Lyons, Phys. Rev. Lett. 36, 1188 (1976).

[30]K. B. Lyons and P. A. Fleury, Solid State Commun. 23, 477 (1977).

[31]S. R. Andrews, R. T. Harley, I. R. Jahn, and W. F. Sherman, J. Phys. C 15, 4679 (1982).

[32]See P. A. Fleury and K. B. Lyons, Solid State Commun. 32, 103 (1979), and references therein.

[33]L. L. Chase, J. Sokoloff, and L. A. Boatner, Solid State Commun. 55, 451 (1985).

[34]Edward Lee, L. L. Chase, and L. A. Boatner, Phys. Rev. B 23, 1438 (1985).

[35]Wu Xing, H. Looser, H. Wuest, and H. Arend, J. Cryst. Growth 78, 431 (1986).

[36]A. M. Quittet, M. I. Bell, M. Krauzman, and P. M. Raccah, Phys. Rev. B 14, 5068 (1976).

[37]D. G. Bozinis and J. P. Hurrel, Phys. Rev. B 13, 3109 (1976).

[38]M. D. Fontana, G. E. Kugel, J. Vamvakas, and C. Carabatos, J. Phys. (Paris) Colloq. 42, C6-749 (1981).

[39]R. Currat, R. Comes, B. Dorner, and E. Wiesendanger, J. Phys. C 7, 2521 (1974).

[40]G. Burns and F. Dacol, Phys. Rev. B 18, 5750 (1978).

[41]J. A. Sanjurjo and R. S. Katiyar, Ferroelectrics 37, 693 (1981).

[42]A. Scalabrin, A. S. Chaves, D. S. Shim, and S. P. S. Porto, Phys. Status Solidi B 79, 731 (1977).

[43]Samples made by Sanders Co. typically have a T_{c1} of $\simeq 130\,°C$, we believe our measured value of $T_{c1} = 124\,°C$ to be the result of a systematic error, and not a reflection on the sample quality which was good.

[44]J. P. Sokoloff, L. L. Chase, and L. A. Boatner (unpublished).

[45]C. A. S. Lima, A. Scalabrin, L. M. C. Miranda, A. Vargas, and S. P. S. Porto, Phys. Status Solidi B 86, 373 (1978).

[46]A. Scalabrin, S. P. S. Porto, H. Vargas, C. A. S. Lima, and L. C. M. Miranda, Solid State Commun. 24, 291 (1977).

[47]T. Scheider and E. Stoll, Phys. Rev. B 31, 1254 (1973).

[48]J. A. Krumhansl and J. R. Schrieffer, Phys. Rev. B 11, 3535 (1975).

[49]A. D. Bruce and T. Schneider, Phys. Rev. B 16, 3991 (1977).

[50]H. Presting, J. A. Sanjurjo, and H. Vogt, Phys. Rev. B 28, 6097 (1983).

[51]G. Kugel, H. Vogt, W. Kress, and D. Rytz, Phys. Rev. B 30, 985 (1984).

[52]R. A. Field, D. A. Gallagher, and M. V. Klein, Phys. Rev. B 18, 2995 (1978).

[53]We have just been made aware of a report by M. D. Fontana, A. Ridah, and G. E. Kugel, J. Phase Transitions (to be published), in which a central peak was observed in KNbO$_3$.